Biointerface Research in Applied Chemistry
Open-Access Journal (ISSN: 2069-5837)

Article
Volume 13, Issue 6, 2023, 508
https://doi.org/10.33263/BRIAC136.508

Complex Formations of Favipiravir and BeO-Decorated Carbon Nanocones along with Quantum Processing

Kun Harismah [1,*], Mahmoud Mirzaei [2,*]

[1] Department of Chemical Engineering, Faculty of Engineering, Universitas Muhammadiyah Surakarta, Surakarta, Indonesia; kun.harismah@ums.ac.id (K.H.);
[2] Child Growth and Development Research Center, Research Institute for Primordial Prevention of Non-Communicable Disease, Isfahan University of Medical Sciences, Isfahan, Iran; mirzaei.res@gmail.com (M.M.);
* Correspondence: kun.harismah@ums.ac.id (K.H.); mirzaei.res@gmail.com (M.M.);

Scopus Author ID 56982926300 (K.H.);
13204227300 (M.M.)

Received: 9.10.2022; Accepted: 24.11.2022; Published: 31.01.2023

Abstract: To the need to develop theoretic treatments for infectious diseases, this work was performed based on quantum processes of complex formations of favipiravir (FAV) antiviral drug and a model of beryllium-oxygen (BeO)-decorated carbon nanocone (BOC). The models were stabilized, and their features were evaluated. Regarding the achievements of optimization calculations, eight models of FAV@BOC complexes were found to affirm the idea of such complex formation between the interacting substances. The models with O…Be, N…Be, and H…O interactions were found at higher strengths of adsorption in comparison with the models with F…Be interactions. Details of interactions indicated a level of physical adsorption for the FAV substance at the tip of the BOC substance with a dominant role of the BeO-decorated region for conducting the adsorption process. Additionally, molecular orbital features indicated significant changes from the singular to complex states, in which the models were able to be recognized based on measurements of such features. In this regard, formations of FAV@BOC complexes were achieved by the benefits of managing the future functions of adsorbed FAV substance, especially for approaching a desired drug delivery purpose.

Keywords: nanocarbon; nanocone; favipiravir; COVID-19; adsorption; quantum calculations.

1. Introduction

Favipiravir is a pyrazine-carboxamide derivative with antiviral activity against influenza and other viral infections [1]. It has become well known, especially soon after the coronavirus disease (COVID-19) appearance in late 2019 [2]. Besides its expected higher efficiency for treating novel influenza infestations compared to the seasonal types of influenza, several attempts have been dedicated to improving it for treating specific viral infections [3-5]. Additionally, the adverse effects of favipiravir medication for the infected patients showed a need to develop more efficient medication methods for this drug [6]. To this aim, earlier works examined the benefits of employing combinations of favipiravir and nanostructures to approach a drug delivery platform [7, 8]. The idea was initiated by the roles of nanostructures for conducting the targeted drug delivery systems to enhance medication efficiency [9-11]. In this case, the nanostructure could work as a carrier for the adsorbed drug to deliver it to the correct target [12-14]. Accordingly, learning details of drug-nanostructure combinations could help to propose a novel carrier/adsorbent for the specified drug [15-17]. This is very important

regarding drug design, discovery, and development to reach an appropriate point of efficient medication [18-20]. Although there are considerable improvements in drug issues, the successes of pharmaceutical treatments are not certain yet [21-23]. Accordingly, several efforts are still required to enhance drug efficiency and rely on pharmaceutical treatments [24-26]. For the cases of nanostructures, several architectures based on different shapes and compositions with specified applications have been identified up to now [27-30]. Accordingly, their modifications with other atomic and molecular substances yielded newly decorated nanostructures [31].

In addition to the pioneering innovation of carbon nanostructures, decorating the original carbon compositions yielded new substances with enhanced features, especially for working as adsorbents towards other substances [32-36]. To this point, a carbon nanocone was investigated in this work to adsorb the favipiravir substance for approaching insights into conducting drug delivery platforms. The apex architecture of conical nanostructures could provide a tip for communicating with other substances [37-39]. Based on such characteristic features, the tip of the employed nanocone was decorated by beryllium and oxygen atoms to create a Be-O-C nanocone for interacting with the favipiravir substance. As shown in Figure 1, the singular models of favipiravir (FAV) and modified nanocone (BOC) were involved in the various configurations of interactions to yield the FAV@BOC complexes, indicated by F1-F8. To generate the required information, quantum processing of molecular models in singular and complex formats was done to optimize the structural geometries and obtain their related features [40-42]. As a consequence, an idea of favipiravir-nanocarbon complex formations was assessed in this work using the quantum processing tools to provide more insights on conducting the drug delivery platforms.

2. Materials and Methods

In Figure 1, the investigated models of this work were exhibited in their singular and complex formats, including favipiravir (FAV), beryllium-oxygen decorated carbon nanocone (BOC), and eight configurations of FAV@BOC complexes, F1-F8. The singular models were optimized to reach their minimized energy geometries, and they were subsequently combined with each other to produce complex models during the optimization of various interacting configurations. Accordingly, eight models were obtained based on the geometrical optimizations of bimolecular models as indicated by F1-F8. Besides performing such optimization calculations, interaction details of complex models were identified using the quantum theory of atoms in molecules (QTAIM) analyses by the MultiWfn software [43, 44]. As included in Table 1, types of interactions (Int.), distances (Dis.), total electron density (ρ), Laplacian of electron density ($\nabla^2\rho$), energy density (H), and energy of formation (E_F) were evaluated for each of the FAV@BOC complexes. Next, further analyses were done by evaluating the molecular descriptors, including the energy of the highest occupied molecular orbital (E_H), the energy of the lowest unoccupied molecular orbital (E_L), the energy gap (E_G), and dipole moment (D_M) (Table 2). To evaluate the required information of this work, density functional theory (DFT) quantum processes were done to optimize the models and obtain their descriptors. The B3LYP-D3/6-31G* level of DFT calculations was performed using the Gaussian program [45]. Next, the models were visualized using the ChemCraft software [46]. It could be briefly described here that the methodology of this work was based on employing computational tools and theories to obtain stabilized structures first and evaluate their features

next. In this regard, computations and visualizations were done to approach the purpose of performing a quantum processing study.

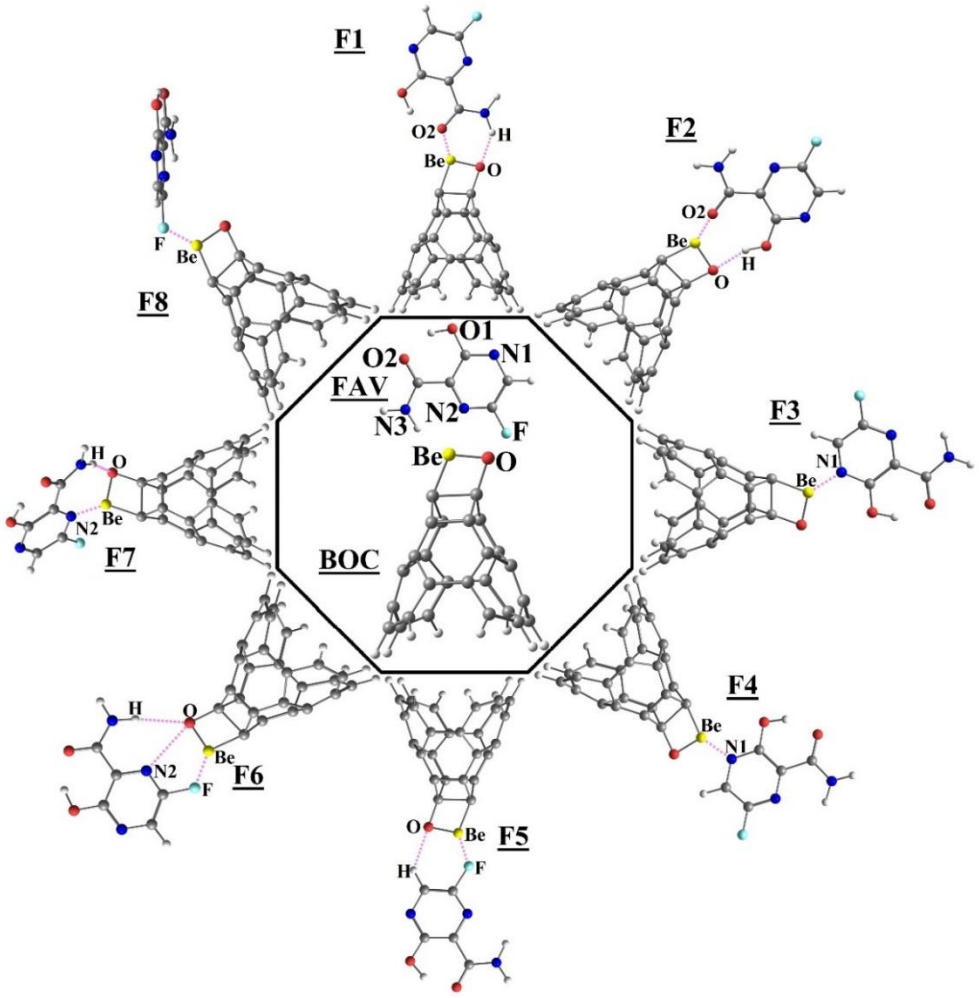

Figure 1. Optimized models of this work, F1 to F8 are the obtained models of FAV@BOC complexes.

Table 1. Interactions descriptors of FAV@BOC models; F1-F8.*

FAV@BOC	Int.	Dis. Å	ρ au	$\nabla^2\rho$ au	H au	E_F kcal/mol
F1	O2…Be	1.571	0.0735	0.6554	0.0194	-47.160
	H…O	1.762	0.0342	0.1267	0.0007	
F2	O2…Be	1.609	0.0715	0.5901	0.0129	-36.392
	H…O	1.791	0.0341	0.1306	0.0005	
F3	N1…Be	1.732	0.0644	0.3948	0.0021	-39.207
F4	N1…Be	1.736	0.0635	0.3927	0.0018	-39.068
F5	F…Be	1.671	0.0472	0.4142	0.0128	-19.100
	H…O	2.191	0.0156	0.0589	0.0011	
F6	F…Be	1.715	0.0419	0.3479	0.0099	-21.206
	N2…O	2.798	0.0141	0.0482	0.0008	
	H…O	2.401	0.0090	0.0329	0.0006	
F7	N2…Be	1.737	0.0638	0.3868	0.0014	-38.006
	H…O	1.799	0.0381	0.1202	-0.0013	
F8	F…Be	1.687	0.0453	0.3897	0.0117	-18.204

*The models are shown in Figure 1.

3. Results and Discussion

The current research work aimed to perform quantum processes on the formations of favipiravir-nanocarbon complexes. As shown in Figure 1, the investigated nanocarbon was a carbon nanocone with Be-O-C composition yielding the BOC substance towards adsorbing the FAV substance. The role of Be-O was to decorate the original carbon composition nanocone

to provide a doped nanostructure for participating in interactions with the FAV substance. It is worth mentioning that the nanostructures with Be-O compositions were reported before [47], and such decoration was done for making a specific region of interactions for the nanocone of this work. On the other hand, formations of complexes of FAV and nanostructures were examined by the earlier works [7, 8], and the combination of FAV and BOC was aimed to be examined in this work. Indeed, the importance of exploring novel treatments for novel viral infections caused the initiation of this work to find the benefits of such complex formations for approaching the delivery purposes of FAV antiviral drugs. To approach the goal, the investigated models were carefully analyzed at their molecular and atomic scales to reveal insights into the formations of FAV@BOC complexes.

F3 and F4 involved one N…Be interaction, in which the strength of that interaction was strong enough to produce a FAV@BOC complex model. Based on Table 1, F3 was found in a slightly higher level of formation strength in comparison with F4, with values of -39.207 and -39.068 kcal/mol, respectively. Comparing the strength of complex formations with F1 and F2 indicated this order: F1 > F3 > F4 > F2. Further analyses of interaction details indicated a higher electronic portion for F3 than F4. The values of each of ρ, $\nabla^2\rho$, and H could help to show the strengths of interactions regarding the electronic portions, in which the models were suitable in the case of physical interactions.

For F5, F6, and F8 complexes, the fluorine atom of FAV was involved in interactions with the BOC substance. As shown in Figure 1, F…Be interaction was found for all of the three mentioned complexes. F8 included only one F…Be interaction, F5 included two F…Be and H…O interactions, and F6 included three F…Be, N2…O, and H…O interactions. Comparing the values of E_F indicated this strength order F6 > F5 > F8 for the models. Details of Table 1 indicated meaningful portions of electrons for the involving interactions, in which substances of the models were in physical modes of interactions. Comparing with other discussed complexes could yield this order of formation strength: F1 > F3 > F4 > F2 > F6 > F5 > F8.

F7 was found with two N…Be and H…O interactions, in which the complex model was stabilized through the involved interactions. The strength of this complex was found to be comparable with those of F1-F4, in which a new order of strength could be defined here: F1 > F3 > F4 > F7 > F2 > F6 > F5 > F8. This model's electronic portions of interactions (Table 1) also affirmed a form of the physical complex. Indeed, interactions of the investigated models were in physical modes of formations with a possibility of conducting a reversible complex formation. In this regard, the models were found strong enough for the formation, and their details of infarctions (Table 1) showed features of electron portions for achieving the targeted FAV@BOC complexes. As a consequence, formations of FAV@BOC complexes were affirmed by the obtained results to this point.

Molecular descriptors of the optimized models were summarized in Table 2 to show the features of molecular orbitals and dipole moments. The results showed significant effects on the molecular orbitals features of the singular FAV model after the complex formation. However, less significance of effects was observed for the molecular orbitals features of the singular BOC model after the complex formation. In this regard, a dominant role of BOC substance for conducting the adsorption process of FAV substance was found, which could also be applied to measure the features to recognize the occurrence of the adsorption process. Not only the adsorption process but also the adsorbed configuration could be achievable in this case. Interestingly, the values of E_H, E_L, and E_G were meaningful differences to be detectable

regarding the occurrence of the adsorption process. In this regard, the models were found suitable to be recognized based on the adsorbed configurations.

Additionally, the calculated values of D_M could reveal the effects of general electronic distribution on the molecular surface. A higher or a lower value could show the way of such an electronic distribution system. Consequently, FAV@BOC complexes were available based on different formation strengths, and their electronic molecular orbitals also affirmed variations of electronic features for the investigated models. Based on measurements of E_G, it could be possible to separate the desired complexes by inserting them in a specified drug delivery platform. Hence, the formation of FAV@BOC complexes could be proposed for conducting a drug delivery process based on the required features of interactions for each of obtained configurations. A protective role of BOC could also be considered for managing the future interactions of the adsorbed FAV substance.

Table 2. Molecular descriptors of FAV, BOC, and FAV@BOC models.*

Model	E_H eV	E_L eV	E_G eV	D_M Debye
FAV	-8.893	-0.523	8.370	3.391
BOC	-7.101	-1.000	6.101	2.572
F1	-6.567	-1.651	4.917	6.079
F2	-6.491	-1.584	4.906	8.254
F3	-6.439	-1.979	4.460	10.079
F4	-6.378	-1.968	4.411	10.021
F5	-6.724	-1.328	5.396	5.494
F6	-6.760	-1.272	5.488	0.459
F7	-6.744	-1.898	4.846	1.338
F8	-6.694	-1.376	5.318	3.221

*The models are shown in Figure 1.

4. Conclusions

The idea of the formation of FAV@BOC complexes was examined in this work by performing quantum processes on the molecular models. The models were optimized, and their features were evaluated to learn the details of such complex formations. The Be-O doped region of nanocone worked as an active site of interactions towards the FAV substance, in which eight complexes were found accordingly. The results indicated different configurations of relaxation for the FAV substance on the BOC surface. Involving O…Be, N…Be, and H…O interactions from FAV to BOC were at the highest level of strength.

On the other hand, involving F…Be and other complementary interactions helped to produce some complexes with lower levels of adsorption strengths. Analyses of molecular orbital features also indicated the benefits of employing BOC for recognizing the adsorbed configuration of FAV, in which the values of EG could help to distinguish the complexes. As a consequence, the models of FAV@BOC complexes were suitable for formation, and they were separable by the molecular orbitals features. A dominant role of protective of FAV was also found for the BOC substance proposing it for employment in a desired drug delivery process.

Funding

This research received a fund (no. 199648) from the Research Council of Isfahan University of Medical Sciences, Isfahan, Iran.

Acknowledgments

This research has no acknowledgment.

Conflicts of Interest

The authors declare no conflict of interest.

References

1. Shiraki, K.; Daikoku, T. Favipiravir, an anti-influenza drug against life-threatening RNA virus infections. *Pharmacology & Therapeutics* **2020,** *209*, 107512, https://doi.org/10.1016/j.pharmthera.2020.107512.
2. Joshi, S.; Parkar, J.; Ansari, A.; Vora, A.; Talwar, D.; Tiwaskar, M.; Patil, S.; Barkate, H. Role of favipiravir in the treatment of COVID-19. *International Journal of Infectious Diseases* **2021,** *102*, 501–508, https://doi.org/10.1016/j.ijid.2020.10.069.
3. Negru, P.A.; Radu, A.F.; Vesa, C.M.; Behl, T.; Abdel-Daim, M.M.; Nechifor, A.C.; Endres, L.; Stoicescu, M.; Pasca, B.; Tit, D.M.; Bungau, S.G. Therapeutic dilemmas in addressing SARS-CoV-2 infection: favipiravir versus remdesivir. *Biomedicine & Pharmacotherapy* **2022,** *147*, 112700, https://doi.org/10.1016/j.biopha.2022.112700.
4. Marlin, R.; Desjardins, D.; Contreras, V.; Lingas, G.; Solas, C.; Roques, P.; Naninck, T.; Pascal, Q.; Behillil, S.; Maisonnasse, P.; Lemaitre, J. Antiviral efficacy of favipiravir against Zika and SARS-CoV-2 viruses in non-human primates. *Nature Communications* **2022,** *13*, 1–10, https://doi.org/10.1038/s41467-022-32565-w.
5. Pilkington, V.; Pepperrell, T.; Hill, A. A review of the safety of favipiravir–a potential treatment in the COVID-19 pandemic?. *Journal of Virus Eradication* **2020,** *6*, 45–51, https://doi.org/10.1016/S2055-6640(20)30016-9.
6. Ergür, F.Ö.; Yıldız, M.; Şener, M.U.; Kavurgacı, S.; Ozturk, A. Adverse effects associated with favipiravir in patients with COVID-19 pneumonia: a retrospective study. *Sao Paulo Medical Journal* **2022,** *140*, 372–377, https://doi.org/10.1590/1516-3180.2021.0489.R1.13082021.
7. Pari, A.A.; Yousefi, M. Interactions between favipiravir and a BNC cage towards drug delivery applications. *Structural Chemistry* **2022,** *33*, 159–167, https://doi.org/10.1007/s11224-021-01833-8.
8. Harismah, K.; Shahrtash, S.A.; Arabi, A.R.; Khadivi, R.; Mirzaei, M.; Akhavan-Sigari, R. Favipiravir attachment to a conical nanocarbon: DFT assessments of the drug delivery approach. *Computational and Theoretical Chemistry* **2022,** *1216*, 113866, https://doi.org/10.1016/j.comptc.2022.113866.
9. Baghernejad, B.; Alikhani, M. Nano-cerium oxide/aluminum oxide as an efficient catalyst for the synthesis of xanthene derivatives as potential antiviral and anti-inflammatory agents. *Journal of Applied Organometallic Chemistry* **2022,** *2*, 155–162, https://doi.org/10.22034/jaoc.2022.154819.
10. Shete, R.; Fernandes, P.; Borhade, B.; Pawar, A.; Sonawane, M.; Warude, N. Review of cobalt oxide nanoparticles: green synthesis, biomedical applications, and toxicity studies. *Journal of Chemical Reviews* **2022,** *4*, 331–345, https://doi.org/10.22034/jcr.2022.342398.1172.
11. Chen L, Hong W, Ren W, Xu T, Qian Z, He Z. Recent progress in targeted delivery vectors based on biomimetic nanoparticles. *Signal Transduction and Targeted Therapy* **2021,** *6*, 1–25, https://doi.org/10.1038/s41392-021-00631-2.
12. Al Samarrai, E.; Alwan, L.H.; Al-Haddad, S.A.H.; Al Samarrai, M.H.; Al-Obaidi, M.; Al Samarrai, O. Spectrophotometric determination of phenobarbital in pharmaceutical preparation using gold nanoparticles. *Eurasian Chemical Communications* **2022,** *4*, 812–825, https://doi.org/10.22034/ecc.2022.329806.1329.
13. Maghsoudi, S.; Hosseini, S.A.; Ravandi, S. A review on phospholipid and liposome carriers: synthetic methods and their applications in drug delivery. *Journal of Chemical Reviews* **2022,** *4*, 346–363, https://doi.org/10.22034/jcr.2022.355104.1182.
14. Manzari, M.T.; Shamay, Y.; Kiguchi, H.; Rosen, N.; Scaltriti, M.; Heller, D.A. Targeted drug delivery strategies for precision medicines. *Nature Reviews Materials* **2021,** *6*, 351–370, https://doi.org/10.1038/s41578-020-00269-6.
15. Pour Karim, S.; Ahmadi, R.; Yousefi, M.; Kalateh, K.; Zarei, G. Interaction of graphene with amoxicillin antibiotic by in silico study. *Chemical Methodologies* **2022,** *6*, 861–871, https://doi.org/10.22034/chemm.2022.347571.1560.

16. Kamel Attar Kar, M.H.; Yousefi, M. Investigating drug delivery of 5-fluorouracil by assistance of an iron-modified graphene scaffold: computational studies. *Main Group Chemistry* **2022,** *21,* 651–658, https://doi.org/10.3233/MGC-210164.
17. Yaraghi, A.; Ozkendir, O.M.; Mirzaei, M. DFT studies of 5-fluorouracil tautomers on a silicon graphene nanosheet. *Superlattices and Microstructures* **2015,** *85,* 784–788, https://doi.org/10.1016/j.spmi.2015.05.053.
18. Ghiasifar, M.; Hosseinnejad, T.; Ahangar, A. Copper catalyzed cycloaddition reaction of azidomethyl benzene with 2,2-di(prop-2-yn-1-yl)propane-1,3-diol: DFT and QTAIM investigation. *Progress in Chemical and Biochemical Research* **2022,** *5,* 1–20, https://doi.org/10.22034/pcbr.2022.319090.1203.
19. Farhami, N. A computational study of thiophene adsorption on boron nitride nanotube. *Journal of Applied Organometallic Chemistry* **2022,** *2,* 163–172, https://doi.org/10.22034/jaoc.2022.154821.
20. Alizadeh, S.; Nazari, Z. Amphetamine, methamphetamine, morphine@AuNPs kit based on PARAFAC. *Advanced Journal of Chemistry-Section A* **2022,** *5,* 253–262, https://doi.org/10.22034/ajca.2022.345350.1318.
21. Mousavi, S.; Zare, S.; Mirzaei, M.; Feizi, A. Novel drug design for treatment of COVID-19: a systematic review of preclinical studies. *Canadian Journal of Infectious Diseases and Medical Microbiology* **2022,** *2022,* 2044282, https://doi.org/10.1155/2022/2044282.
22. Saroyo, H.; Saputri, N.F. Cytotoxicity of mangrove leaves (rhizophora) ethanolic extract on cancer cells. *Journal of Nutraceuticals and Herbal Medicine* **2021,** *4,* 43–52, https://doi.org/10.23917/jnhm.v4i1.15657.
23. Mohseniabbasabadi, T.; Behboodyzad, F.; Abolhasani Zadeh, F.; Balali, E. Vismodegib anticancer drug: analyzing electronic and structural features and examining biological activities. *Main Group Chemistry* **2022,** *21,* 631–40, https://doi.org/10.3233/MGC-210160.
24. Fathi, A.; Rismanchian, M.; Dezaki, S.N. Effectiveness of different antimicrobial agents on malodor prevention in two-stage dental implants: a double-blinded randomized clinical trial. *European Journal of Dentistry* **2022,** *in press,* https://doi.org/10.1055/s-0042-1747954.
25. Saliminasab, M.; Jabbari, H.; Farahmand, H.; Asadi, M.; Soleimani, M.; Fathi, A. Study of antibacterial performance of synthesized silver nanoparticles on Streptococcus mutans bacteria. *Nanomedicine Research Journal* **2022,** *7,* 391–396, https://doi.org/10.22034/nmrj.2022.04.010.
26. Hudiyawati, D.; Syafitry, W. Effectiveness of physical and psychological treatment for cancer-related fatigue: systematic review. *Jurnal Kesehatan* **2021,** *14,* 195–211, https://doi.org/10.23917/jk.v14i2.15596.
27. Wang, J.; Li, Y.; Nie, G. Multifunctional biomolecule nanostructures for cancer therapy. *Nature Reviews Materials* **2021,** *6,* 766–783, https://doi.org/10.1038/s41578-021-00315-x.
28. Kareem, T.A.; Mahdi, D.K. Synthesis and characterization of silver nanoparticles-doped mesoporous bioactive glass prepared by spray pyrolysis. *Eurasian Chemical Communications* **2022,** *4,* 330–337, https://doi.org/10.22034/ecc.2022.326506.1311.
29. Hamid Abd, A.; Adnan Ibrahim, O. Synthesis of carbon quantum dot by electro-chemical method and dtudying optical, electrical, and structural properties. *Chemical Methodologies* **2022,** *6,* 823–830, https://doi.org/10.22034/chemm.2022.351559.1575.
30. Sukmawati, A.; Utami, W.; Yuliani, R.; Da'I, M.; Nafarin, A. Effect of tween 80 on nanoparticle preparation of modified chitosan for targeted delivery of combination doxorubicin and curcumin analogue. *IOP Conference Series: Materials Science and Engineering* **2018,** *311,* 012024, https://doi.org/10.1088/1757-899X/311/1/012024.
31. Darougari, H.; Rezaei-Sameti, M. The drug delivery appraisal of Cu and Ni decorated B12N12 nanocage for an 8-hydroxyquinoline drug: A DFT and TD-DFT computational study. *Asian Journal of Nanosciences and Materials* **2022,** *5,* 196–210, http://www.ajnanomat.com/article_154625.html.
32. Mehrabi Nasab, D.; Taheri, A.; Athari, S.S. Conjugation of cortistatin peptide with gold nanoparticles synthesized to investigate anti-inflammatory effects in allergic asthma. *Journal of Medicinal and Chemical Sciences* **2023,** *6,* 20–28 https://doi.org/10.26655/JMCHEMSCI.2023.1.3.
33. Jalali Sarvestani, M.R. TNT interaction with BN Nanocone: a comprehensive computational study. *Journal of Medicinal and Chemical Sciences* **2020,** *3,* 317–328, https://doi.org/10.26655/jmchemsci.2020.4.1.
34. Wikantyasning, E.R.; Mutmainnah, M.; Ramadhan, G.; Cholisoh, Z.; Da'i, M. Preparation of poly (acrylic acid) crosslinked-gold nanoparticles for colorimetric detection of analytes. *Materials Science Forum* **2019,** *950,* 138–143, https://doi.org/10.4028/www.scientific.net/MSF.950.138.
35. Hassani, M.; Zeeb, M.; Monzavi, A.; Khodadadi, Z.; Kalaee, M.R. Response surface modeling and optimization of microbial fuel cells with surface-modified graphite anode electrode by ZSM-5 nanocatalyst

functionalized. *Chemical Methodologies* **2022,** *6*, 253–268, https://doi.org/10.22034/chemm.2022.324312.1425.
36. Golipour-Chobar, E.; Salimi, F.; Ebrahimzadeh-Rajaei, G. Sensing of lomustine drug by pure and doped C48 nanoclusters: DFT calculations. *Chemical Methodologies* **2022,** *6*, 790–800, https://doi.org/10.22034/chemm.2022.344895.1555.
37. Harismah, K.; Mirzaei, M.; Dai, M.; Roshandel, Z.; Salarrezaei, E. In silico investigation of nanocarbon biosensors for diagnosis of COVID-19. *Eurasian Chemical Communications* **2021,** *3*, 95–102, https://doi.org/10.22034/ecc.2021.267226.1120.
38. Charlier, J.C.; Rignanese, G.M. Electronic structure of carbon nanocones. *Physical Review Letters* **2001,** *86*, 5970, https://doi.org/10.1103/PhysRevLett.86.5970.
39. Kose, A.; Yuksel, N.; Fellah, M.F. Hydrogen adsorption on Ni doped carbon nanocone. *Diamond and Related Materials* **2022,** *124*, 108921, https://doi.org/10.1016/j.diamond.2022.108921.
40. Zinner, M.; Dahlhausen, F.; Boehme, P.; Ehlers, J.; Bieske, L.; Fehring, L. Quantum computing's potential for drug discovery: early stage industry dynamics. *Drug Discovery Today* **2021,** *26*, 1680–1688, https://doi.org/10.1016/j.drudis.2021.06.003.
41. Mohamed, H.; Hamza, Z.; Nagdy, A.; El-Mageed, H. Computational studies and DFT calculations of synthesized triazolo pyrimidine derivatives: a review. *Journal of Chemical Reviews* **2022,** *4*, 156–190, https://doi.org/10.22034/jcr.2022.325439.1138.
42. Isvandi, M.; Ravaei, B.; Alizadeh, R. Chemical computers and computing based on chemical reactions: current status and outlook. *Advanced Journal of Chemistry-Section A* **2022,** *5*, 311–319, https://doi.org/10.22034/ajca.2022.360288.1329.
43. Cortés-Guzmán, F.; Bader, R.F. Complementarity of QTAIM and MO theory in the study of bonding in donor–acceptor complexes. *Coordination Chemistry Reviews* **2005,** *249*, 633–662, https://doi.org/10.1016/j.ccr.2004.08.022.
44. Lu, T.; Chen, F. Multiwfn: a multifunctional wavefunction analyzer. *Journal of Computational Chemistry* **2012,** *33*, 580, https://doi.org/10.1002/Jcc.22885.
45. Frisch, M.J.; Trucks, G.W.; Schlegel, H.B.; Scuseria, G.E.; Robb, M.A.; Cheeseman, J.R. Gaussian 09 program. *Gaussian Inc.* Wallingford, CT, **2009**, https://www.gaussian.com.
46. ChemCraft. https://www.chemcraftprog.com.
47. Jasim, S.A.; Yasin, G.; Ansari, M.J.; Zarifi, K. Density functional theory investigation of ozone gas uptake by a BeO nanoflake. *Main Group Chemistry* **2022,** *21*, 773–781, https://doi.org/10.3233/MGC-210147.